Behavior of the Two-Dimensional Viscous Flow over Two Circular Cylinders with Different Radii

Surattana Sungnul and Ekkachai Kunnawuttipreechachan

***Abstract*—In this paper, we study numerical simulation of two-dimensional viscous flow over two circular cylinders with different radii. The flow structure depends on the rate of rotation, the gap-spacing and the Reynolds number. The algorithm used to simulate the numerical solutions is based on the concept of projection method. A mathematical model describing the flow over the two rotating cylinders is applied by the cylindrical bipolar coordinate system. The main objective is to investigate the characteristics of the fluid flow. This investigation gives a set of numerical simulations for the hydrodynamic characteristics, which can be applied to other related problems.**

***Index Terms*—numerical simulation, cylindrical bipolar coordinate, projection method.**

I. Introduction

THE interaction of the flow over two cylinders is a topic of prime scientific interest with many engineering and real life applications. Most of researches studied on two cylinders were concerned with two rotating and non-rotating cylinders of an identical diameter (see for example [1]- [4] and literature cited there). There are two different types of stationary motion of bodies in a fluid. The first type is a towed body which in the stationary motion regime external forces must affect the body. The second type is self-propelled body. Self-propelled means that a body moves because of the interaction between its boundary and the surrounding fluid and without the action of an external force. In the present work, flow structures were calculated between two circular cylinders (the left cylinder is non-rotating and the right cylinder is rotating in counterclockwise angular velocity) with different radii and uniform stream flow directed perpendicular to the line connecting the cylinders centers. We show some results of numerical simulations at fixed Reynolds number and moderate gap spacing and rate of cylinders rotation.

II. Mathematical Modelling

The governing equation is the Navier-Stokes equations written in cylindrical bipolar coordinate. The coordinate system is moving together with the cylinders. The cylindrical bipolar coordinate system can be defined by the following equation (1)

$$x = \frac{a \sinh \eta}{\cosh \eta - \cos \xi}, \quad y = \frac{a \sin \xi}{\cosh \eta - \cos \xi}, \tag{1}$$

Manuscript received December 28, 2017; revised January 25, 2018. This research was financially supported by the Faculty of Applied Science, King Mongkut's University of Technology North Bangkok (Contract no. 5642110).

Surattana Sungnul is a lecturer at the Department of Mathematics, King Mongkut's University of Technology North Bangkok, 10800, THAILAND and a researcher in Centre of Excellence in Mathematics, CHE, Bangkok, 10400, THAILAND e-mail: surattana.s@sci.kmutnb.ac.th

Ekkachai Kunnawuttipreechachan is a lecturer in the Department of Mathematics, King Mongkut's University of Technology North Bangkok, 10800, THAILAND e-mail: ekkachai.k@sci.kmutnb.ac.th

where $\xi \in [0, 2\pi)$, $\eta \in (-\infty, \infty)$, a is a characteristic length in the cylindrical bipolar coordinate system which is positive. This transformation maps the $xy-$ plane (form which the domain occupied by the cylinders is excluded) into the rectangle $\eta_2 \leq \eta \leq \eta_1, \quad 0 \leq \xi < 2\pi$ and $\eta_2 < 0$, $\eta_1 > 0$. The surfaces of the cylinders are located at $\eta = \eta_2$ and $\eta = \eta_1$. The cylinder's radii r_1, r_2 and the distance of their centers from the origin d_1, d_2 are given by $r_i = a \operatorname{csch}|\eta_i|, \quad d_i = a \coth|\eta_i|, \quad i = 1, 2$. The center to center distance between the cylinders is $d = d_1 + d_2$.
The Navier-Stokes equations (2)-(4) in the cylindrical bipolar coordinate system (ξ, η) [5] are

$$\frac{\partial v_\xi}{\partial t} + \frac{1}{h}\left(v_\xi \frac{\partial v_\xi}{\partial \xi} + v_\eta \frac{\partial v_\xi}{\partial \eta}\right) - \\ -\frac{1}{a}\left(\sinh\eta(v_\xi v_\eta) - \sin\xi(v_\eta)^2\right) = -\frac{1}{h}\frac{1}{\rho}\frac{\partial p}{\partial \xi} + \\ +\frac{\nu}{h}\left\{\frac{1}{h}\left(\frac{\partial^2 v_\xi}{\partial \xi^2} + \frac{\partial^2 v_\xi}{\partial \eta^2}\right) - \frac{2}{a}\left(\sinh\eta\frac{\partial v_\eta}{\partial \xi} - \sin\xi\frac{\partial v_\eta}{\partial \eta}\right) \\ -\left(\frac{\cosh\eta + \cos\xi}{a}\right)v_\xi\right\}, \tag{2}$$

$$\frac{\partial v_\eta}{\partial t} + \frac{1}{h}\left(v_\xi \frac{\partial v_\eta}{\partial \xi} + v_\eta \frac{\partial v_\eta}{\partial \eta}\right) + \\ +\frac{1}{a}\left(\sinh\eta(v_\xi)^2 - \sin\xi(v_\xi v_\eta)\right) = -\frac{1}{h}\frac{1}{\rho}\frac{\partial p}{\partial \eta} + \\ +\frac{\nu}{h}\left\{\frac{1}{h}\left(\frac{\partial^2 v_\eta}{\partial \xi^2} + \frac{\partial^2 v_\eta}{\partial \eta^2}\right) + \frac{2}{a}\left(\sinh\eta\frac{\partial v_\xi}{\partial \xi} - \sin\xi\frac{\partial v_\xi}{\partial \eta}\right) \\ -\left(\frac{\cosh\eta + \cos\xi}{a}\right)v_\eta\right\}, \tag{3}$$

$$\frac{1}{h^2}\left(\frac{\partial(hv_\xi)}{\partial \xi} + \frac{\partial(hv_\eta)}{\partial \eta}\right) = 0, \tag{4}$$

where v_ξ and v_η are the physical components of velocity vector $v = (v_\xi, v_\eta)$, p is the pressure, ρ is density, ν is the kinematic viscosity of the fluid and $h = \dfrac{a}{(\cosh\eta - \cos\xi)}$.
The boundary conditions are a no-slip requirement on cylinders

$$v_\xi = \omega_i r_i, \quad v_\eta = 0, \text{ on } \eta = \eta_i, \ \xi \in [0, 2\pi), \ i = 1, 2, \tag{5}$$

where $\omega_i, \quad i = 1, 2$ are constant angular velocities of the cylinders rotation. Positive values of $\omega_i, \quad i = 1, 2$ correspond to counterclockwise rotation. Upstream and downstream boundary conditions at infinity are

$$v_x = 0, \quad v_y = U_\infty, \quad \text{as } r^2 = x^2 + y^2 \to \infty, \tag{6}$$

where v_x and v_y are components of velocity vector in x and y directions respectively and U_∞ is the oncoming free

ISBN: 978-988-14047-8-7
ISSN: 2078-0958 (Print); ISSN: 2078-0966 (Online)

stream velocity. The net force and torque exerted by fluid on an immersed body with surface Σ are

$$\mathbf{F} = \int_{\mathbf{\Sigma}} \tau \, \mathbf{dS}, \quad \mathbf{M} = \int_{\mathbf{\Sigma}} [\mathbf{r} \times \tau] \mathbf{dS},$$

where n is the unit vector normal to the Σ that points outside the region occupied by the fluid. The force per unit area exerted across a rigid boundary element with normal n in an incompressible fluid is defined by

$$\tau = -p\, n - \mu(n \times \omega)$$

where ω is vorticity defined as $\omega = curl\ v$ and μ is the coefficient of viscosity. If F_{x_i} and F_{y_i}, $i = 1, 2$ are the lift and drag on the cylinders, the lift and drag coefficients are defined by

$$C_{L_i} = \frac{F_{x_i}}{\rho U_\infty D}, \ C_{D_i} = \frac{F_{y_i}}{\rho U_\infty D}, i = 1, 2, \qquad (7)$$

where D is a diameter of right cylinder and each consists of components due to the friction forces and the pressure. Hence

$$C_L = C_{Lf} + C_{Lp}, \ C_D = C_{Df} + C_{Dp}. \qquad (8)$$

The problem of self-motion is to find solution of the Navier-Stokes equations (2)-(4) with boundary conditions $(5) - (6)$ and additional constraints

$$\mathbf{F} = \mathbf{M} = \mathbf{0}. \qquad (9)$$

Equation (9) determines the basic distinction between stationary flow over self-propelled and towed bodies. The numerical simulation of the flow past self-moving bodies becomes more complicated as a result of the nonlocality of constraints like (9). For such flows, the results depend not only on the Reynolds number, Re, but also depend on the non-dimensional gap spacing between the two cylinders, g, and parameters, α_i representing the ratios of the rotational velocities of the cylinder walls to the oncoming flow velocity

$$Re = \frac{U_\infty\, D}{\nu}, \ \alpha_i = \frac{D\omega_i}{2U_\infty}, \ i = 1, 2, \ \text{and} \ g = \frac{d - r_1 - r_2}{D/2}.$$

III. Numerical Algorithm and Validation

The algorithm of the problem solution is based on the concept of projection methods (Chorin, 1968) [6]. The intermediate velocity components $\tilde{v_\xi}, \tilde{v_\eta}$ are computed in a first step by solving a finite difference approximation of the momentum equations. Intermediate velocity vector $\widetilde{v}$ (which is not solenoidal) is then decomposed into divergence free and rotational free vector fields by solving Poisson equation with homogeneous Neumann boundary conditions. The final approximation of the v and p at time t^{n+1} can be found and the steady-state computed solution is defined by

$$\frac{\|\theta^{n+1} - \theta^n\|}{\triangle t \|\theta^{n+1}\|} \leq \varepsilon,$$

where $\theta = (v_\xi,\ v_\eta,\ C_D,\ C_L)$; $\triangle t$ is the time step and θ^n refers to the numerical approximation at time $n\triangle t$.

To validate the present numerical algorithm, the uniform flow past rotating circular cylinders with $Re = 20,\ 0.1 \leq \alpha_1 (= \alpha_2) \leq 2.0$ and a large gap between cylinder surfaces $g = 14$ have been calculated and the results compared with simulation data for flow past a single cylinder. All the simulations have been performed in a large domain so as to reduce the influence of the outer boundary. Tables I and II list drag and lift coefficients from our calculation and makes a comparison with (Ingham et al. 1990) [7], (Badr et al. 1989) [8] and (Chung 2006) [9]. It can be seen that the differences are acceptable for C_D and C_L. The analysis of the data collected in Tables I and II indicate an acceptable level of agreement between our computational results and the experimental and numerical data available in literature.

TABLE I
Drag coefficient of flow over a rotating circular cylinder at $Re = 20$ with gap spacing $g = 14$

Contribution	C_D		
	$\alpha = 0.1$	$\alpha = 1.0$	$\alpha = 2.0$
Present	2.119	1.887	1.363
Badr *et al.* [8]	1.990	2.000	—
Ingham and Tang [7]	1.995	1.925	1.627
Chung [9]	2.043	1.888	1.361

TABLE II
Lift coefficient of flow over a rotating circular cylinder at $Re = 20$ with gap spacing $g = 14$

Contribution	C_L		
	$\alpha = 0.1$	$\alpha = 1.0$	$\alpha = 2.0$
Present	0.291	2.797	5.866
Badr *et al.* [8]	0.276	2.740	—
Ingham and Tang [7]	0.254	2.617	5.719
Chung [9]	0.258	2.629	5.507

TABLE III
Drag coefficients of flow over two circular cylinders at fixed $Re = 20,\ \alpha_2 = 0.0$ and $g = 1.0, 2.0, 3.0$ for $1.0 \leq \alpha_1 \leq 6.0$

g	α_1	C_D	C_{D_1}	C_{D_2}
1.0	1.0	5.903	2.239	3.664
	2.0	3.662	0.581	3.081
	4.0	0.279	-1.603	1.882
	4.25	**0.009**	-1.550	1.559
	5.0	-0.417	-1.489	1.072
2.0	1.0	6.344	2.576	3.768
	2.0	4.656	1.212	3.444
	4.0	1.160	-1.111	2.271
	5.0	**0.002**	-1.434	1.436
	6.0	-1.185	-0.936	-0.249
3.0	1.0	6.217	2.678	3.539
	2.0	4.552	1.354	3.198
	4.0	1.343	-0.856	2.199
	5.5	**−0.007**	-1.157	1.150
	6.0	0.498	-0.473	0.971

IV. Numerical Results

In this work, two cylinders are placed in a stream of the uniform speed U_∞ at infinity. Numerical results have been presented into two parts. In the first part, the left cylinder with radius 2 is non-rotating, whiles the right cylinder with radius 1 is rotating in anti-clockwise angular velocity. The influence of the rotation rate α_1 is demonstrated in Tables III and IV. The values of drag and lift coefficients in case of fixed Reynolds number, $Re = 20$ and various gap spacing, $g = 1.0, 2.0, 3.0$ for $1.0 \leq \alpha_1 \leq 6.0$ are shown in Tables

ISBN: 978-988-14047-8-7
ISSN: 2078-0958 (Print); ISSN: 2078-0966 (Online)

TABLE IV
LIFT COEFFICIENT OF FLOW OVER TWO CIRCULAR CYLINDERS AT FIXED $Re = 20,\ \alpha_2 = 0.0$ AND $g = 1.0, 2.0, 3.0$ FOR $1.0 \leq \alpha_1 \leq 6.0$

g	α_1	C_L	C_{L_1}	C_{L_2}
1.0	1.0	2.805	5.104	-2.299
	2.0	6.204	8.322	-2.118
	4.0	16.944	17.770	-0.826
	4.25	18.526	19.100	-0.574
	5.0	24.130	24.110	0.020
2.0	1.0	4.070	4.610	-0.540
	2.0	7.035	8.342	-1.307
	4.0	17.059	17.950	-0.891
	5.0	24.461	24.720	-0.259
	6.0	28.728	28.410	0.318
3.0	1.0	4.924	4.343	0.581
	2.0	7.560	8.076	-0.516
	4.0	17.432	17.800	-0.368
	5.5	28.570	28.590	-0.020
	6.0	33.376	33.290	0.086

III and IV. The drag coefficients of both cylinders decrease with increasing α_1, at fixed g, (see in the third column of Table III). The lift coefficients of both cylinders increase with increasing α_1, at fixed g, as shown in the third column of Table IV. We found that in the case of fixed Reynolds number, $Re = 20$, rate of rotation corresponding to zero drag force $(\tilde{\alpha_1})$ increases when g increases. For example, Table III shows that at $Re = 20,\ \tilde{\alpha_1}$ corresponding to zero drag force are $\tilde{\alpha_1} \approx 4.25,\ (g = 1.0)$, $\tilde{\alpha_1} \approx 5.0,\ (g = 2.0)$ and $\tilde{\alpha_1} \approx 5.5,\ (g = 3.0)$. The streamline patterns from the simulations are shown in Fig.1- Fig.3 . The streamline patterns and pressure contours in the case rate of rotation corresponding to zero drag force $(\tilde{\alpha_1})$ are occurred for $g = 1.0, 2.0, 3.0$ with respectively (see in Fig. 2).

In the second part, the left cylinder is rotating $\alpha_2 = 1.0$ and the right cylinder is rotating in counterclockwise angular velocity. The effect of the rotation rate α_1 is demonstrated in Tables V and VI. The values of drag and lift coefficients in the case of fixed Reynolds number, $Re = 20$ and various gap spacing, $g = 1.0, 2.0, 3.0$ for $1.0 \leq \alpha_1 \leq 6.0$ are also shown. The drag coefficients of both cylinders decrease with increasing α_1, at fixed g, (see in the third column of Table V). The lift coefficients of both cylinders increase with increasing α_1, at fixed g, as shown in the third column of Table VI. The simulations of streamline patterns are shown in Fig.4 - Fig.6. This work is a fundamental problem which can be applied to some classes of obstructed flow.

V. CONCLUSION AND SUGGESTION

Numerical results show the flow structure over two rotating circular cylinders with different radii depend on the rate of rotation, the gap spacing and the Reynolds number. We found that at fixed gap spacing g, the drag coefficient of both cylinders decrease with increasing α and the lift coefficient of both cylinders increase with increasing α. In addition we obtain the rate of rotation corresponding to zero drag force $(\tilde{\alpha_1})$ increases when g increases at fixed $Re = 20$. However these results $(\tilde{\alpha_1})$ are not the numerical solutions of self-motion regime because its satisfy only $C_D \approx 0$ but C_L is not close to zero. Numerical solutions of flow over multiple cylinders can be used the projection method with the finite difference method but the governing equations

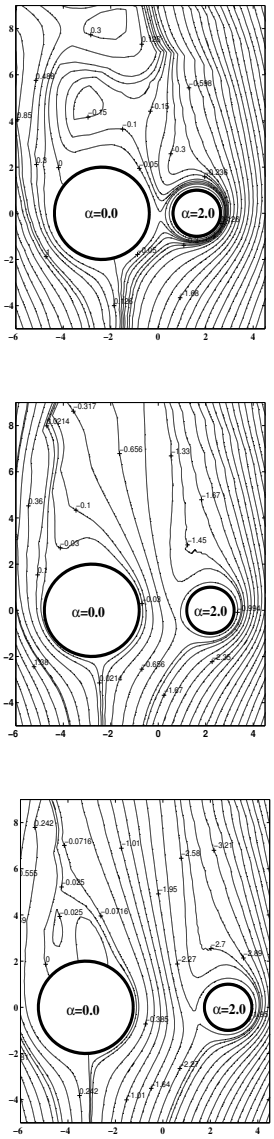

Fig. 1. streamline patterns of flow over two circular cylinders at $Re = 20, g = 1.0,\ 2.0,\ 3.0$ and $\alpha_1 = 2.0,\ \alpha_2 = 0.0$.

TABLE V
DRAG COEFFICIENTS OF FLOW OVER TWO CIRCULAR CYLINDERS AT FIXED $Re = 20,\ \alpha_2 = 1.0$ AND $g = 1.0, 2.0, 3.0$ FOR $1.0 \leq \alpha_1 \leq 6.0$

g	α_1	C_D	C_{D_1}	C_{D_2}
1.0	1.0	9.886	3.037	6.849
	2.0	6.958	1.343	5.615
	4.0	2.902	-0.924	3.826
	6.0	1.543	-0.324	1.867
2.0	1.0	8.528	2.344	6.184
	2.0	6.376	0.888	5.488
	4.0	2.106	-1.270	3.376
	6.0	0.994	-0.510	1.504
3.0	1.0	8.632	2.623	6.009
	2.0	7.432	1.482	5.950
	4.0	4.410	0.066	4.344
	6.0	1.565	-0.355	1.920

ISBN: 978-988-14047-8-7
ISSN: 2078-0958 (Print); ISSN: 2078-0966 (Online)

TABLE VI
LIFT COEFFICIENTS OF FLOW OVER TWO CIRCULAR CYLINDERS AT FIXED $Re = 20,\ \alpha_2 = 1.0$ AND $g = 1.0, 2.0, 3.0$ FOR $1.0 \leq \alpha_1 \leq 6.0$

g	α_1	C_L	C_{L_1}	C_{L_2}
1.0	1.0	5.988	5.974	0.014
	2.0	9.965	10.360	-0.395
	4.0	21.765	22.110	-0.345
	6.0	39.713	39.010	0.703
2.0	1.0	7.218	4.774	2.444
	2.0	10.396	8.795	1.601
	4.0	21.040	19.660	1.380
	6.0	37.257	35.780	1.477
3.0	1.0	10.069	4.677	5.392
	2.0	13.600	8.959	4.641
	4.0	24.659	20.570	4.089
	6.0	39.565	36.430	3.135

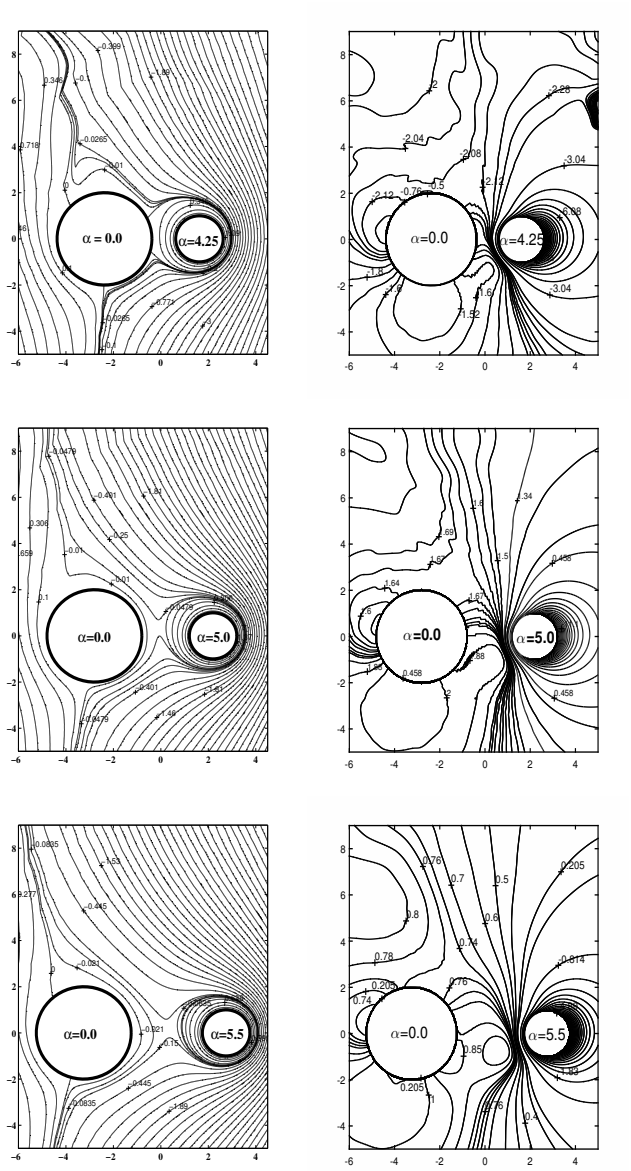

Fig. 2. Streamline patterns and Pressure contours of flow over two circular cylinders at $Re = 20,\ \tilde{\alpha_1} = 4.25\ (g = 1.0),\ \tilde{\alpha_1} = 5.0\ (g = 2.0),\ \tilde{\alpha_1} = 5.5\ (g = 3.0)$ and $\alpha_2 = 0.0$

have to transform to another coordinate system. In addition, numerical solutions of fluid flow over two rotating circular cylinders for self-motion regime with different radii and in cases of higher Reynolds numbers may be investigated for future works.

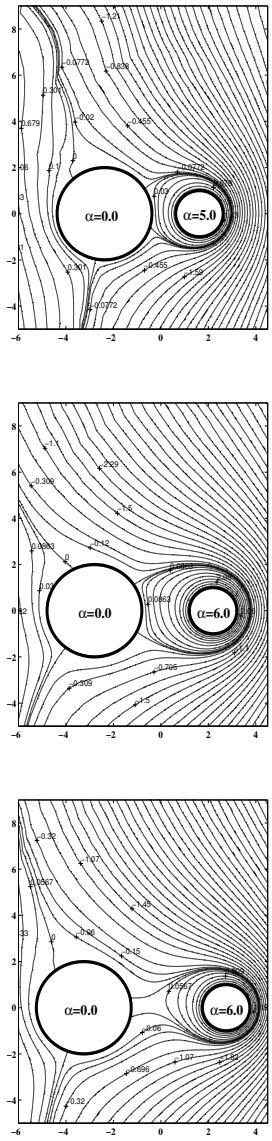

Fig. 3. streamline patterns of flow over two circular cylinders at $Re = 20,\ \alpha_1 = 5.0\ (g = 1.0),\ \alpha_1 = 6.0\ (g = 2.0),\ \alpha_1 = 6.0\ (g = 3.0)$ and $\alpha_2 = 0.0$

ACKNOWLEDGMENT

We would like to thanks the Faculty of Applied Science, King Mongkut's University of Technology North Bangkok for supporting us in doing this work.

REFERENCES

[1] M. M. Zdravkovich, "Review of Flow Interference between Two Circular Cylinders in Various Arrangements," *ASME J. Fluids Eng.*, vol. 99, pp. 618-633, 1977.
[2] S. Kang, "Characteristics of Flow over Two Circular Cylinders in a Side-by-Side Arrangement at Low Reynolds Numbers," *Phys. of Fluids*, vol. 15, no. 9, pp. 486-498, 2003.
[3] S. Sungnul and N. P. Moshkin, "Numerical Simulation of Flow over Two Rotating Self-Moving Circular Cylinders," *Recent Advances in Computational Sciences*, World Scientific Publishing-Imperial College Press, pp. 278-296, 2008.

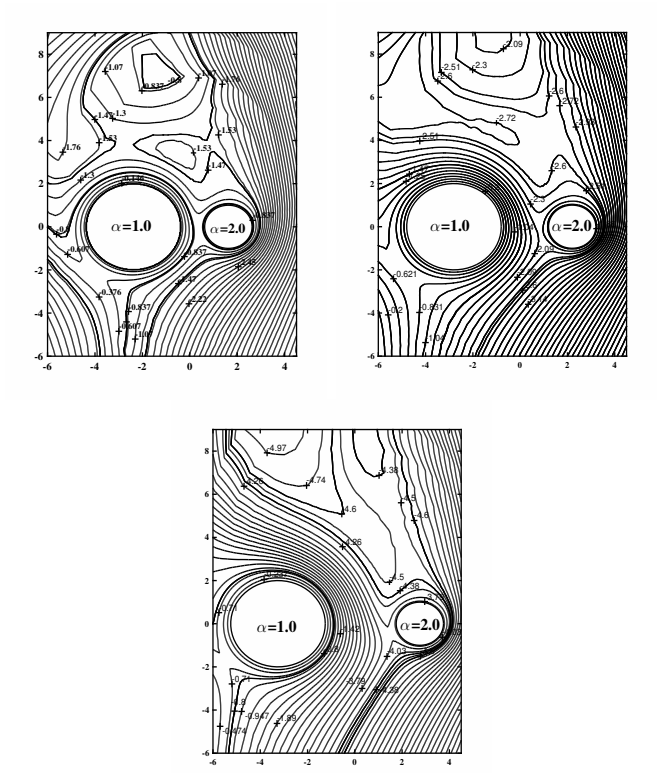

Fig. 4. streamline patterns of flow over two circular cylinders at $Re = 20, g = 1.0,\ 2.0,\ 3.0$ and $\alpha_1 = 2.0,\ \alpha_2 = 1.0$.

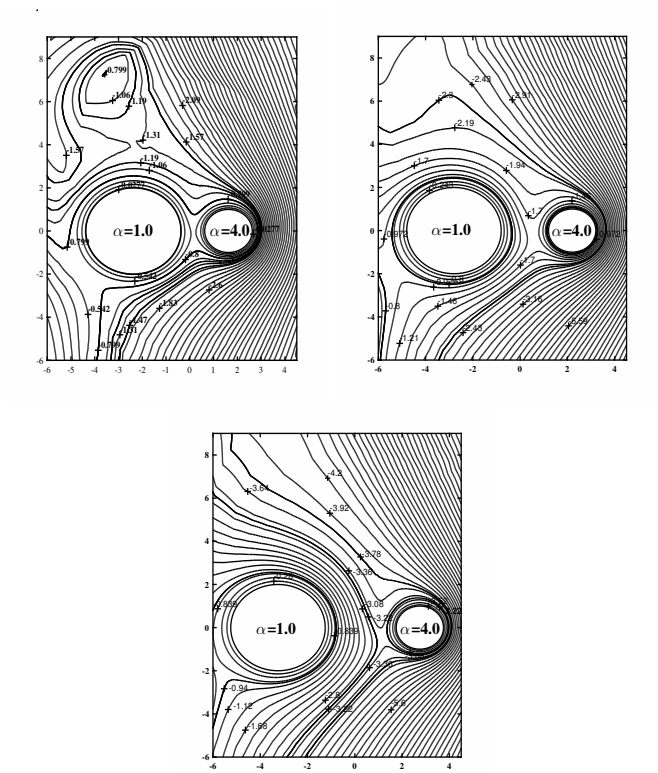

Fig. 5. streamline patterns of flow over two circular cylinders at $Re = 20, g = 1.0,\ 2.0,\ 3.0$ and $\alpha_1 = 4.0,\ \alpha_2 = 1.0$.

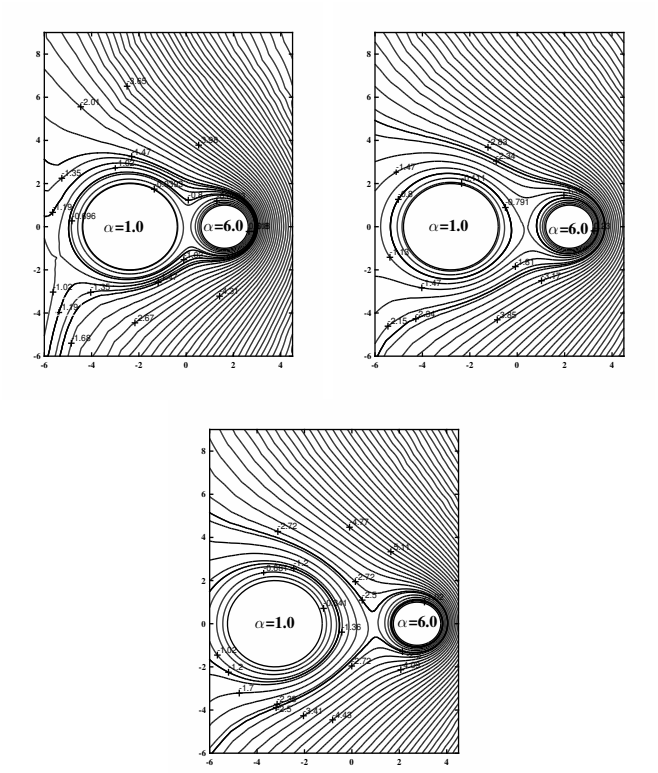

Fig. 6. streamline patterns of flow over two circular cylinders at $Re = 20, g = 1.0,\ 2.0,\ 3.0$ and $\alpha_1 = 6.0,\ \alpha_2 = 1.0$.

[4] S. K. Panda, "Two-Dimensional Flow of Power-Law Fluids over a Pair of Cylinders in Side-by-Side Arrangement in the Laminar Regime," *Braz. J. Chem. Eng.*, vol. 34, no. 2, pp. 507-530, 2017.

[5] S. Sungnul, "On the Representation of the Navier-Stokes Equations in Cylindrical Bipolar Coordinate System," in *Proceedings in Annual National Symposium on Computational Science and Engineering 2005*, pp. 340-348.

[6] S. J. Chorin, "Numerical Solution of the Navier-Stokes Equations," *Math. Comp.*, vol. 22, pp. 745-762, 1968.

[7] D. B. Ingham and T. Tang, "A Numerical Investigation into the Steady Flow past a Rotating Circular Cylinder at Low and Intermediate Reynolds Numbers," *Journal of Computational Physics*, vol. 87, pp. 91-107, 1990.

[8] D. Badr, S. C. R. Dennis and P. J. S. Young, "Steady and Unsteady Flow past a Rotating Cylinder at Low Reynolds Numbers," *Computer and Fluids*, vol. 17, no. 4, pp. 579-609, 1989.

[9] M-H. Chung, "Cartesian Cut Cell Approach for Simulating Incompressible Flows with Rigid Bodies of Arbitrary Shape," *Computer and Fluids*, vol. 35, no. 6, pp. 607-623, 2006.

ISBN: 978-988-14047-8-7
ISSN: 2078-0958 (Print); ISSN: 2078-0966 (Online)